32nd Annual International Conference of the IEEE EMBS
Buenos Aires, Argentina, August 31 - September 4, 2010

Probing Protein Binding Spectra with Fourier Microfluidics

C. H. Mastrangelo, *Member, IEEE*, L. D. Williams and T. Ghosh

***Abstract*—New developments in microfluidic chip technology enable the construction of chemical spectrum analyzers that can probe the binding interactions between chemical entities. In this paper we report the implementation of a microfluidic chip suitable for Fourier transform measurements of biochemical interactions. The chip consists of a chemical signal generator, a flow cell and a binding sensor surface. The microfluidic signal generator produces a periodic stream of protein plugs in solution flowing at constant velocity through the cell. This flow produces periodic association and dissociation cycles of the protein to a functionalized gold sensing surface placed inside the cell. The sensor activity corresponding to the phasor response of the chemical interaction at the excitation frequency is measured optically using surface plasmon resonance (SPR) imaging. We demonstrated the feasibility of the technique using a model system of carbonic anhydrase-II (CA-II) and immobilized 4-(2-Aminoethyl) benzenesulfonamide (ABS) ligand. The observed transfer function showed a dominant pole at 10.2 mHz corresponding to association and dissociation constants of 4.8 x 10^3 $M^{-1}\cdot s^{-1}$, and 3.5 x 10^{-2} s^{-1} respectively.**

I. Introduction

THE quantitative characterization of interactions between two or more biomolecules is essential to scientific and technological progress in drug discovery, pharmacokinetics, systems biology and food science. In drug discovery millions of small molecule compounds are tested by pharmaceutical companies every year against scores of protein targets. In bio-defense the detection of weak interactions between a low concentration agent and a particular biological receptor can be a matter of life or death, and in clinical applications, the selective detection of low levels of oncogenic protein markers can be crucial for early cancer detection and treatment.

The most common chemical interaction is the binding of two molecular entities. In chemical binding measurements one of the molecules can be immobilized on a surface (a ligand) while exposed to its binding partner in solution (an analyte). More complex reactions may involve multiple and intermediate species mediated by enzymes. Present experimental techniques [1-3] for binding measurements involve fitting of a recorded time-domain binding sensor signal (or *sensorgram*) to a model response. This methodology thus requires *a-priori* knowledge of the reaction dynamics, the number of species involved and the order of the reaction. The assumed model information is however not required if one treats the biochemical reaction as a general dynamical system under test as shown in the block diagram below

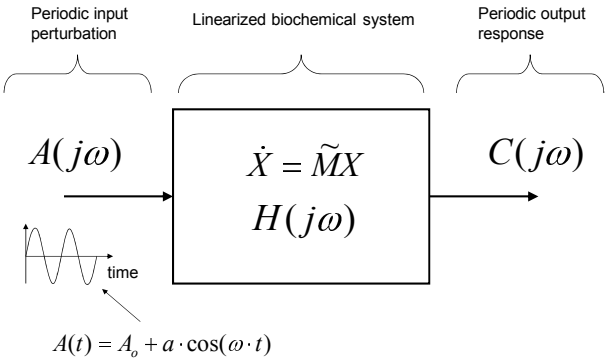

Fig. 1: The biochemical reaction under test can be abstracted as a general dynamical system that can be excited with input chemical signals. The system response under periodic excitation is its transfer function.

The biochemical system can be probed by introducing different chemical excitation input signals and observing its binding sensorgram response. In particular, if the input excitation is periodic and sinusoidal, the observed response is the frequency response of its transfer function

$$H(j\omega) = \frac{C(j\omega)}{A(j\omega)} \quad . \tag{1}$$

The (observable) dynamics can thus be identified from the pole and zero distribution of its frequency response. With this scheme one can thus implement a chemical binding spectrum analyzer where the input chemical entity signal is swept in frequency while recording the frequency dependent sensorgram response.

II. Probing The Binding Spectra

The simplest biochemical interaction is the first order reaction of Eq. (2) where two reacting species A and B form a product C with corresponding association and dissociation constants k_a and k_d

$$A + B \underset{k_d}{\overset{k_a}{\rightleftharpoons}} C \tag{2}$$

The concentration of the product C follows the first order reaction dynamics specified by the ordinary differential equation shown in Eq. (3)

Manuscript received April 1, 2010.

C. H. Mastrangelo is with the Electrical Engineering and Bioengineering Departments, University of Utah, Salt Lake City, UT 84112 (e-mail: carlos.mastrangelo@utah.edu).

L. D. Williams is with the Electrical Engineering Department, University of Utah, Salt Lake City, UT 84112 (e-mail: layne.williams@utah.edu).

T. Ghosh is with the Bioengineering Department, University of Utah, Salt Lake City, UT 84112 (e-mail: t.ghosh@utah.edu).

$$\frac{dC}{dt} = k_a \cdot (B_o - C) \cdot A - k_d \cdot C \tag{3}$$

where B_o is the surface concentration of the undisturbed immobilized ligand, A is the analyte (volumetric) concentration in solution and C is the surface concentration of the ligand-analyte product. It is easily shown using perturbation analysis of Eq. (3) that under small input analyte sinusoidal excursions $\hat{a} \cdot e^{j\omega t}$ about fixed concentration A_o, the product also has corresponding fixed and sinusoidal components C_o and $\hat{c} \cdot e^{j\omega t}$. The (complex) transfer function $H(j\omega)$ and its corresponding sensorgram follow

$$H(j\omega) = \frac{C(j\omega)}{A(j\omega)} = \frac{\bar{c}}{\hat{a}} = \frac{k_a \cdot B_o}{(k_d + k_a \cdot A_o)} \cdot \frac{1}{(1 + j\omega / p_1)} \tag{4}$$

Eq. (4) displays a single pole behavior with pole p_1

$$p_1 = k_d + k_a \cdot A_o \tag{5}$$

Therefore we can directly relate the kinetic constants of the reaction to the observed pole.

Similarly if the analyte is a mixture of dilute (non-saturating) independent analytes in solution

$$M_T(t) = \sum_{i=1}^{N} \alpha_i A_i(t) \tag{6}$$

each analyte reacting with the sensor surface with characteristic transfer function $H_i(j\omega)$, the observed total transfer function is

$$H_T(j\omega) = \sum_{i=1}^{N} \alpha_i H_i(j\omega) = \sum_{i=1}^{N} \frac{\alpha_i \kappa_i}{(1 + j\omega / p_i)} \tag{7}$$

Then the binding of each independent analyte could be identified by its characteristic pole contribution provided that the poles are sufficiently spaced apart. Furthermore, the leading factor κ_i is an indicator of the binding affinity of each component as shown in the Bode plot of Fig. 2.

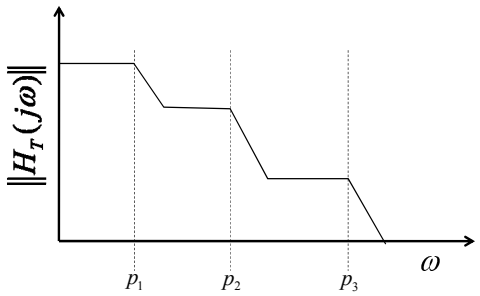

Fig. 2: Example Bode plot for the multi-analyte model transfer function of Eq. (7). The number of independent analytes and the corresponding binding affinity can be identified from the poles of the observed transfer function.

In order to implement this spectral measurement technique it is necessary to generate and transport a stream of analyte plugs to the sensing site with minimal distortion for the entire frequency range of the scan. While this approach is theoretically straightforward there are severe difficulties associated with the signal generation and transmission. A practical scheme can only be realized within the microscopic channels available in microfluidic chips as discussed below.

III. Dispersion of Chemical Signals in Flow Cells

The transmission of solute signals in pressure driven flows is subject to Taylor dispersive mixing which broadens and diffuses the solute plugs as they travel from the signal generator to the sensing site. The net effect of Taylor dispersion is a large enhancement of the solute diffusion. The effective Taylor-dispersion adjusted diffusion coefficient D_{eff} in rectangular capillaries is approximately [4]

$$D_{eff} \cong D_0 \cdot \left(1 + \frac{\alpha(w,h) \cdot V^2}{D_0^2}\right) \tag{8}$$

where α is a function of the width w and height h of the flow capillary [5]

$$\alpha(w,h) \cong \frac{1}{210} \cdot \left[\frac{8.5 \cdot h^2 \cdot w^2}{h^2 + 2.4 \cdot h \cdot w + w^2}\right] \tag{9}$$

D_0 is the intrinsic solute diffusion coefficient and V is the average flow velocity. For mm-sized channels and average velocities of a few cm/s the diffusion enhancement factor is enormous, often reaching values of 10^7 or higher; thus precluding any signal transport in macroscopic implementations. The enhancement factor decreases quadratically with capillary diameter.

The transmission of periodic chemical signals through dispersive channels produces a low-pass characteristic filter behavior [5,6]. The filter transmission pole is

$$p_t \approx \left[\frac{V^3}{D_{eff} \cdot L}\right]^{1/2} \tag{10}$$

where L is the flow cell channel distance between the signal generator and the sensor site. Any excitation signal passing through a capillary element with $\omega > p_t$ will have greatly reduced amplitude. The pole determines the maximum frequency that can be applied to the input sweep. For example a typical microfluidic flow cell 5 mm long with rectangular cross section of $10\times25\mu m^2$, a solute with $D_0=10^{-9}$ m^2/s flowing at a velocity of 5 cm/s yields a transmission cut off pole of 11.5 Hz. In contrast for a flow cell with $1000\times1000\mu m^2$ cross section, 1 cm length at the same velocity the cut off frequency is a much lower 0.1 Hz. The difference in the pole illustrates that the technique is only viable in microfluidic environments.

IV. Test Chip Implementation

We fabricated the microfluidic test chip shown in Fig. 3 to demonstrate the chemical spectrum measurement. The chip consists of two analyte plug generators and two flow cells. Each flow cell has several gold surface plasmon resonance (SPR) [1-3] sensing and reference sites placed along the channels. There are two sets of channels in each chip, one to act as a reference (control) and the other for detection of the

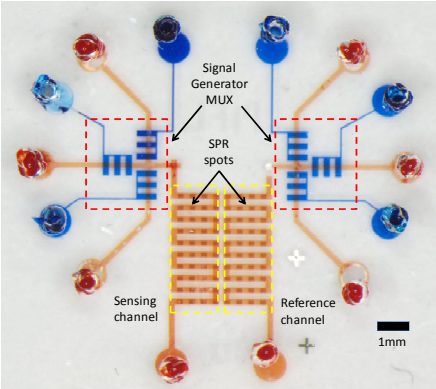

Fig. 3: Photograph of the PDMS microfluidic test chip consisting of two flow multiplexers (signal generators) and two sensing and reference channels. The multiplexer valves are driven by clock ϕ producing periodic association and dissociation steps at the sensing sites.

analyte of interest (sensor). The two channel arrangement is used because it facilitates the functionalization of the reference and sensing sites.

Each plug generator consists of a three-valve flow multiplexer. Two of the valves switch between pure buffer and analyte analyte flows. The third valve is used for regeneration of the sensor surfaces. The analyte/buffer valves are driven by digital clock signals ϕ and $\overline{\phi}$ pulsed at a specific frequency. The test chip was fabricated using conventional two-level PDMS technology [7] with gold patterned sites on the underlying glass. Details of the fabrication and spot functionalization are discussed in the sections below.

V. Materials and Methods

A. Chip Fabrication

SF10 glass substrates in a 2x2" square were purchased from Schott glass. These were chosen to match the SF10 prism used in the SPR readout system. The glass is cleaned by piranha etch (3:1, H_2SO_4:H_2O_2) for 20 minutes, rinsed for 5 min in 18 MΩ de-ionized (DI) water, and dried under N_2. The substrates are placed in an oven at 80 °C for 10 minutes before being transferred to a sputter deposition system. A 3 nm adhesion layer of Ti/W is deposited, followed by 40 nm of gold. The metal layers on the substrate are patterned using photolithography to make an array of 140 x 180 μm rectangles. The metals are etched and the samples rinsed thoroughly with 18 MΩ DI water after each etch step to prevent contamination. Finally, the photoresist is removed and the patterned substrates are stored in a desiccator until used.

B. Chip assembly

Before assembly of the microfluidic chips the patterned glass substrates are further cleaned by flame annealing with a butane micro torch. This is followed with ultrasonic cleaning in methanol for five minutes. The methanol is replaced with fresh solution and the substrate sonicated a total of three times. The dual layer PDMS channels are drilled to make through holes for fluid access, and then cleaned with acetone, IPA, and DI water. The PDMS is dried with an air gun and then baked for 10 minutes on a hot plate at 100 °C, followed by a cooling step for 10 minutes. At this point, both the glass substrate and PDMS channels are placed in the oxygen plasma cleaner for 12 seconds at 400 mTorr oxygen pressure and 25 W power. The assembled chip is baked, again for 10 minutes at 100 °C.

C. Surface Plasmon Resonance Imaging System

A GWC Technologies SPRimager®II system was used to collect the data. The system was modified by the manufacturer to be used in a horizontal configuration, with a custom built microfluidic mounting cell. We further modified the instrument with an 805 nm laser, a Navitar Zoom 6000 lens system, and a Hamamatsu C9100 EMCCD camera.

VI. Protein Binding Experiments

We tested the spectrum analyzer chip concept using a simple protein-binding surface system consisting of carbonic anhydrase-II (CA-II) analyte and an immobilized self-assembled monolayer of 4-(2-Aminoethyl) benzenesulfonamide (ABS) ligand, similar to that used by Lahiri [8]. For this system the transfer function should display the dominant pole behavior of Eq. (3). Prior to the experiment the SPR gold sensing sites are functionalized as discussed below. Prior the spectral measurement we also perform a conventional single-cycle association-dissociation step on the same chip and determine the kinetic constants using a conventional SPR response exponential fit.

A. SPR Spot Functionalization

Surface chemistry modification is performed *in situ* after the chip assembly. The assembled chip is connected to a syringe pump and flushed with 0.01 M HCl for 5 minutes to remove any contaminants or oxide, followed by a 15 minute rinse with DI water. A mixture of long and short chain polyethylene glycol (PEG) molecules is used to provide both a capture surface and one that is protein resistant, following the protocol described by Uchida [9]. A 5 kDa carboxymethyl-PEG-thiol molecule from Laysan Bio is introduced to the flow channels for 20 minutes, followed by a 0.05 M NaOH rinse. Then a 2 kDa methoxy-PEG-thiol is passed through the channels and rinsed similarly. The smaller PEG is applied a total of three times to backfill any gaps in the initial PEG layer and prevent protein adsorption on the gold surface. The surface is again treated with 0.01 M HCl and rinsed with DI water to ensure the proper chemical functionality for the next step. A chemical modification of the carboxy-terminated PEG chains is performed using sulfo-*N*-hydroxysuccinimide (S-NHS) and *N*-ethyl-*N'*-(3-dimethylaminopropyl)carbodiimide (EDC) to create an amine reactive surface. S-NHS at 100 mM and EDC at 400 mM in water are mixed 1:1 and passed through both the reference and sensing channels for 30 minutes. The system is rinsed with phosphate buffered saline (PBS) for two minutes, and then the capture molecule, ABS, is immobilized only to the sensor surface while buffer alone is passed over the reference surface. This illustrates the need for the dual channel system to create a control. Finally, both surfaces are

blocked with ethanolamine at pH 9 for 30 minutes and rinsed with PBS.

B. Experiments

With the chemistry in place the assembled chip is mounted in the SPR system cell. The valves are actuated by a pressure system at 30 psi and controlled by a computer program that sweeps the multiplexer valve clock frequency. Syringes containing analyte, CA-II, at 11.0 μM (330 μg/mL) concentration and buffer are pressurized as well with a constant source at 10 psi which corresponds to a flow rate of 16 cm/s. Experiments are performed by running multiple cycles of a square wave input at different frequencies, from 2 to 260 mHz, as swept by the computer controlled system. Wasabi camera control software from Hamamatsu is used to analyze the collected data by selecting multiple sensing and reference spots in the image. The mean intensity value in each spot is determined for all of the frames in the experiment.

VII. Results and Discussion

Fig. 4 shows an example sensorgram of the frequency sweep from 2 to 260 mHz, at a CA-II concentration of 11.0 μM. Fourier transform analysis is used to determine the magnitude of the transfer function $\|H(j\omega)\|$ at the excitation frequency. $\|H(j\omega)\|$ is next plotted versus each excitation frequency as shown in the Bode plot of Fig. 5. From this plot we can determine the characteristic roll-off pole which corresponds to the first order kinetics of the biochemical

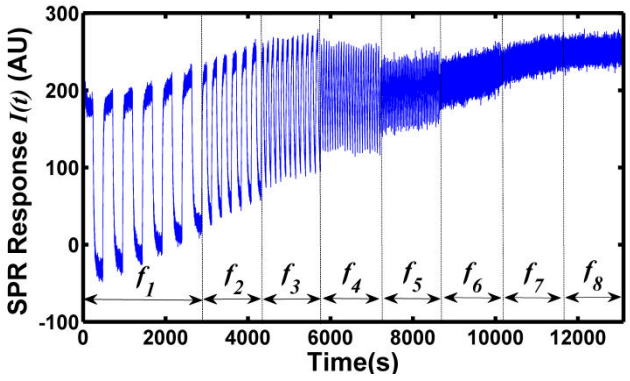

Fig. 4: SPR sensorgram waveform for 11.0 μM CA-II concentration experiment showing the frequency sweep from 2 to 260 mHz.

reaction under test. For this experiment the pole frequency $f_{p1}=p_1/2\pi$ occurs near a frequency of 10.2 mHz. We also performed a conventional single-step conventional SPR response fit analysis on the chip surfaces. The results of the single-step measurement yield fitted values of k_a and k_d for this surface of 4.8 x 10^3 $M^{-1}s^{-1}$ and 3.5 x 10^{-2} s^{-1} respectively. The pole calculated from the single-step fitted constants for this yields a value of f_p = 14.0 mHz at this concentration in reasonable agreement with the pole of the frequency sweep.

While the method described in the paper demonstrates the equivalence of time-domain and frequency-domain measurements, in its present form the swept frequency scheme requires a much longer time than that of the conventional method. It is possible to compress the measurement time using broader spectral test signals. This advanced subject is reserved for our future work.

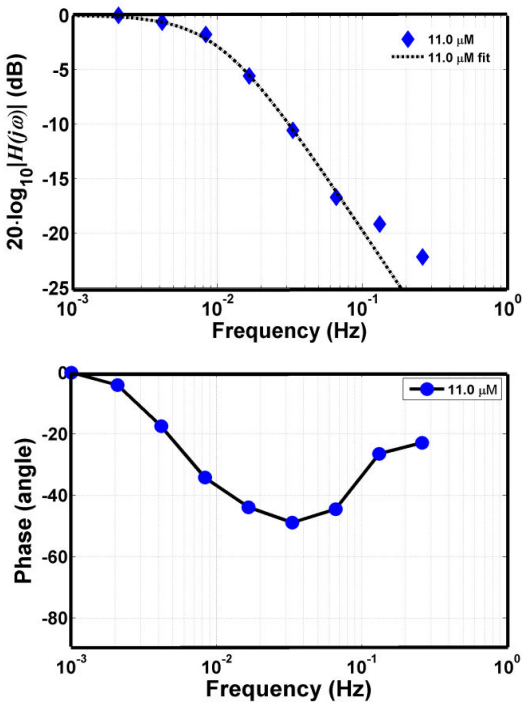

Fig. 5: Bode plots from the 11.0 μM CA-II concentration experiment showing magnitude and phase of the biochemical system frequency response.

VIII. Conclusion

We demonstrated a chip capable of measuring chemical binding spectra of a biochemical interaction. This permits measurement of binding kinetics from frequency response. Using this chip we measured the binding kinetics of a CA-reactive PEG test surface with characteristic role-off pole of 10.2 mHz consistent with the single step calculated value of f_p = 14.0 mHz for the concentration used in the experiment.

IX. References

[1] U. Jönsson, et al., "Real-time biospecific interaction analysis using surface plasmon resonance and a sensor chip technology," *BioTechnique*s, vol. 11, pp. 620-627, 1991.

[2] R.L. Rich, et al., "Kinetic analysis of estrogen receptor ligand interactions," *PNAS*, vol. 99, no. 13, pp. 8562-8567, 2002.

[3] D.G. Myszka, "Analysis of small-molecule interactions using Biacore S51 technology," *Anal. Biochem*., vol. 329, pp. 316-324, 2004.

[4] D. Dutta and D. T. leighton Jr., "Dispersion reduction in pressure-driven flow through microetched channels," *Anal. Chem*.**,** vol. 73, pp. 504-513, 2001.

[5] Y. Xie, Y. Wang, L. Chen and C. H. Mastrangelo, "Fourier microfluidics," *Lab Chip*, vol. 8, pp. 779-785, 2008.

[6] F. Azizi and C. H. Mastrangelo, "Generation of dynamical chemical signals with pulse coded modulators," *Lab Chip*, vol. 8, pp. 907-912, 2008

[7] T. Thorsen, S. J. Maerkl and S. Quake, "Microfluidic large-scale integration," *Science*, vol 239, pp. 580-584, 2002.

[8] J. Lahiri, L. Isaacs, B. Brzybowski, J.D. Carbeck, and G.M. Whitesides,
"Biospecific binding of carbonic anhydrase to mixed SAMs presenting benzenesulfonamide ligands: a model system for studying lateral steric effects," *Langmuir*, vol. 15, pp 7186-7198, 1999.

[9] K. Uchida, H. Otsuka, M. Kaneko, K. Kataoka, and Y. Nagasaki, "A reactive poly(ethylene glycol) layer to achieve specific surface plasmon resonance sensing with a high S/N ratio: the substantial role of a short underbrushed PEG layer in minimizing nonspecific adsorption," *Anal. Chem.*, vol. 77, no. 4, pp 1075–1080, 2005.